

# Energy Spectra of H and He from the ATIC-2 Experiment

J.P. Wefel<sup>a</sup>, J.H. Adams<sup>b</sup>, H.S. Ahn<sup>c</sup>, G.L. Bashindzhagyan<sup>g</sup>, K.E. Batkov<sup>g</sup>,  
J. Chang<sup>d,e</sup>, M. Christl<sup>b</sup>, A.R. Fazely<sup>f</sup>, O. Ganel<sup>c</sup>, R.M. Gunasingha<sup>f</sup>, T.G. Guzik<sup>a</sup>,  
J. Isbert<sup>a</sup>, K.C. Kim<sup>c</sup>, E.N. Kouznetsov<sup>g</sup>, M.I. Panasyuk<sup>g</sup>, A.D. Panov<sup>g</sup>, W.K.H. Schmidt<sup>d</sup>,  
E.S. Seo<sup>c</sup>, N.V. Sokolskaya<sup>g</sup>, J. Wu<sup>c</sup> and V.I. Zatsepin<sup>g</sup>

(a) Louisiana State University, Baton Rouge, LA, USA

(b) Marshall Space Flight Center, Huntsville, AL, USA

(c) University of Maryland, College Park, MD, USA

(d) Max Plank Institute for Solar System Research, Lindau, Germany

(e) Purple Mountain Observatory, Chinese Academy of Sciences (CAS), China

(f) Southern University, Baton Rouge, LA, USA

(g) Skobeltsyn Institute of Nuclear Physics, Moscow State University, Moscow, Russia

Presenter: J. P. Wefel (wefel@phunds.phys.lsu.edu), usa-wefel-J-absl-og11-oral

The Advanced Thin Ionization Calorimeter (ATIC) experiment measures the energy spectra of individual elements, from H to Fe, in the energy region from about 100 GeV to tens of TeV. ATIC was flown twice on long-duration balloon flights around the South Pole, 12/00-1/01 (ATIC-1), and 12/02-1/03 (ATIC-2). Energy deposit spectra for H and He from both flights are presented. The data from ATIC-2 (18 days) show superior resolution and preliminary analysis indicates evolving energy spectra (i.e. becoming harder with increasing energy) consistent with changes expected from propagation models. The data also suggest a slightly steeper source spectrum for H than for He.

## 1. Introduction

The ATIC spectrometer, its calibration, event trajectory reconstruction, use of the Si-matrix for charge determination and the resulting charge resolution have been described elsewhere [1-3]. The ATIC-1 flight was an initial test flight for the instrument, while ATIC-2 was the first science flight. "Lessons learned" from ATIC-1 allowed significant improvements to the experiment which were implemented in the ATIC-2 flight and subsequent data analysis. Preliminary results on H and He spectra from both the ATIC-1 test flight and the ATIC-2 science flight have been presented [4-6]. Since those reports, the temperature dependence of the full instrument response has been measured in a thermal chamber [7], a new spectrum deconvolution procedure has been developed [8], and refined detector calibrations have been applied to ATIC-2. In this progress report we compare the raw energy deposit spectra from the two flights and analyze ATIC-2 through the first version of the deconvolution algorithm. Although still preliminary, the results show evidence for changes in the shape of the energy spectra throughout this high energy region.

## 2. Energy Deposit Spectra and Deconvolution

Figure 1 compares un-normalized energy deposit spectra from ATIC-1 (left) and ATIC-2 (right) for both H (top) and He (bottom) after geometry cuts. Solid symbols show all re-constructed trajectories while open symbols show the spectra with a cut on the trajectory "goodness of fit" parameter. For energy deposits between ~100 and 1,000 GeV, ATIC-1 and ATIC-2 are in agreement within the errors. Above 1 TeV, however, ATIC-1 shows a drop in both the H and He spectra and for both trajectory cuts. This is the region of transition between two gain ranges in the calorimeter, and we are currently re-investigating the ATIC-1 inter-range calibrations. ATIC-2 shows no such effect. In addition, ATIC-2 has been independently cali-

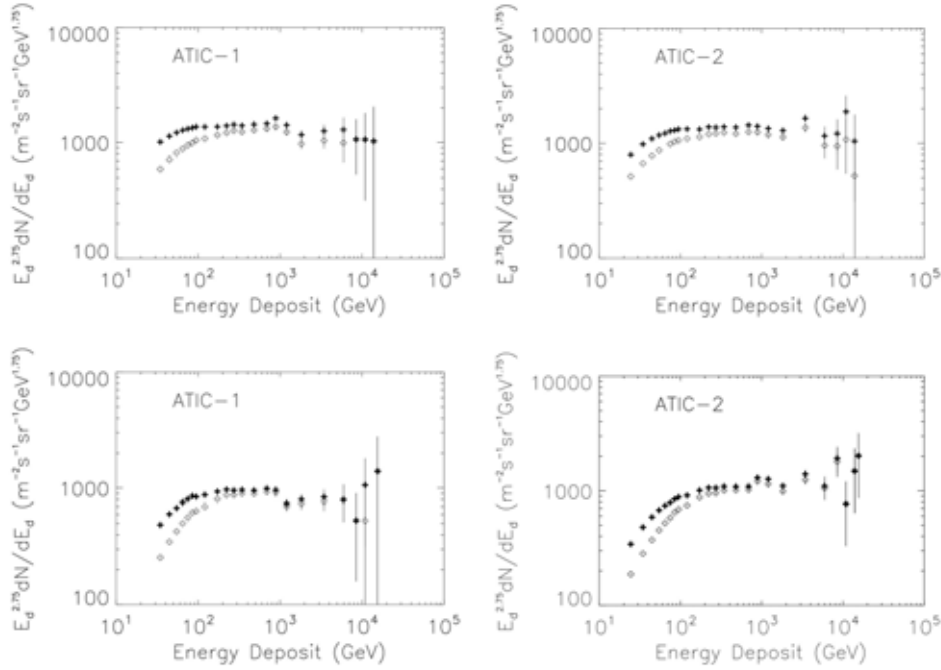


**Figure 1.** Energy deposit spectra (un-normalized) for ATIC-1 (left) and ATIC-2 (right); for H (top) and He (bottom), each for two trajectory reconstruction cuts.

brated, and the data processed, by two different institutions, yielding energy deposit spectra that are in good agreement.

The energy calibration for ATIC is based on careful pre-flight muon calibration of each BGO crystal coupled with in-flight measurements of the inter-range relationship between the three gain ranges for each BGO electronics channel. The accuracy of these calibrations is estimated as  $\pm 5\%$ . The temperature dependence has the form:  $E_{d,corr} = E_d / (1 + 0.0263 \times (T_{calibr} - T_{flight}(t)))$ , where  $E_d$  is the energy deposit determined from the pre-flight muon calibrations,  $T_{calibr}$  is the temperature during the muon calibration,  $T_{flight}(t)$  is current temperature during the flight, and  $E_{d,corr}$  is the temperature corrected energy deposit.

To convert the energy deposit spectra measured in the thin ATIC calorimeter to primary energy spectra, it is necessary to unfold the instrument response, i.e. deconvolve the spectra. In a power law approximation, the measured  $E_d$  spectrum will be steeper than the primary energy ( $E_o$ ) spectrum due to the small increase in leakage from the bottom of the calorimeter as  $E_o$  increases. In addition, a particle interaction at any  $E_o$  results in a distribution of  $E_d$  values, and this distribution is modeled with FLUKA [9] to produce a response matrix  $A(E_o, E_d)$ . Each element of this matrix is, in essence, the probability that a primary particle of energy  $E_o$  incident on the ATIC aperture produces an energy deposit of  $E_d$ .

There is evidence [10-13] that the primary spectra are not simple power laws throughout the high energy region, due to an expected change in the energy dependence of the escape length, for example in the Leaky Box propagation model. (ATIC was designed to search for such effects into the TeV energy region.) Therefore, we do not use the power-law approximation in our deconvolution, but must invert the response matrix as described in [8]. In this context, the response matrix includes effects such as the probability that the incident particle will interact and produce a shower and the energy deposit restrictions applied to the analyzed data. Once these “restored” number of primaries have been obtained the absolute fluxes are calculated by correcting for the geometry factor, the live time, analysis efficiencies, charge resolution, etc. In addition, we

correct for attenuation in the residual atmosphere above the balloon (1.07 for H and 1.18 for He).

### 3. Results and Comparisons

The Leaky Box is a popular empirical model that stands out because of its simplicity. In the application to the case of stable energetic nuclei, the Leaky Box equations can be derived as an approximation to the equations obtained in the flat-halo diffusion model without reacceleration. In this case the simple Leaky Box model predicts a cosmic ray spectrum in the Galaxy,  $N_p(E)$ , as:

$$N_p(E) = \frac{Q_p(E) \times \tau_{esc}(R)}{1 + \lambda_{esc}(R) / \lambda_p} \quad (1)$$

where  $Q_p(E)$  is the source spectrum,  $R$  is magnetic rigidity,  $\tau_{esc}(R) = \lambda_{esc}(R) / (v \times \rho)$ ;  $\lambda_p$  is the interaction length for a particle of type  $p$ ;  $v$  is the particle velocity; and  $\rho$  is the density of the interstellar medium. The energy dependence of the escape length is determined then by the energy dependence of cosmic ray diffusion coefficient  $D$ :  $\lambda_{esc} \propto v/D$ . Results from HEAO-3-C2 [14] for energies below 35 GeV/n and for nuclei heavier than He indicate that  $\lambda_{esc}(R) = 34.1 \times R^{-0.6} \text{ g/cm}^2$  at  $R > 4.4 \text{ GV}$  and  $Q_p(E) \propto E^{-\alpha}$ , where  $\alpha = 2.23$ . This predicts a high energy power law spectrum with spectral index of  $\sim 2.8$ .

Figure 2 (left) shows the  $E_d$  spectra that were used in the first version of the deconvolution. The data were analyzed in an identical fashion to the way the  $A(E_o, E_d)$  matrix was produced by simulations, except the deconvolution only treats five energy bins per decade. Note that both the H (filled) and He (open) spectra do indicate an energy dependence into the TeV region. The right panel of Figure 2 shows the deconvolved spectra compared to previous data. The energy spectra depart from the Leaky Box prediction (curves 1 and 3), showing less steep spectra, as would be expected if the energy dependence of the escape length is changing.

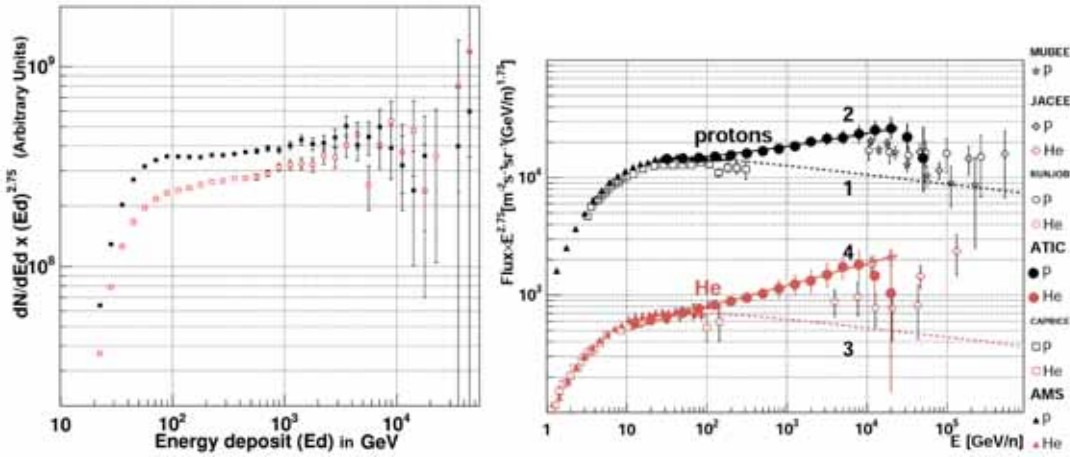


**Figure 2.** ATIC-2 energy deposit spectra (left) for H (top) and He (bottom) used as input to the deconvolution calculation; preliminary deconvolved primary energy spectra (right) compared to previous data [(MUBEE (15); JACEE (16); RUNJOB (17); CAPRICE (18); AMS (19))] and to model calculations.

Osborne and Ptuskin [12] have shown that the form of equation (1) is also correct for a diffusion model with weak reacceleration due to cyclotron resonance scattering of the particles, if  $\lambda_{esc}$  is replaced with an effective

thickness  $x_{eff}$  of the following form:  $x_{eff}(R) = 4.2 \times (R/R_0)^{-1/3} \times (1 + (R/R_0)^{-2/3}) \text{ g/cm}^2$  where  $R_0 = 5.5 \text{ GV}$ . The  $x_{eff}$  parameter models the contribution of diffusive escape and reacceleration in the overall balance of Cosmic rays in the Galaxy. At high rigidities,  $x_{eff} \propto R^{-1/3}$ , expected for Kolmogorov turbulence. Using  $x_{eff}$  in Eq. 1 produces curves 2 and 4 in Figure 2 (right). We can see that the diffusion model with weak reacceleration fits the spectra up to the region above 10 TeV/n where ATIC runs out of events. However, to reproduce the H results, the source spectral index had to be increased from  $\alpha=2.23$  (He) to  $\alpha=2.30$  (H), indicating a difference in the H and He source spectra consistent with JACEE [11].

Figure 2 shows only the initial attempt at deconvolving the measured  $E_d$  spectra. We must still study the effects of different analysis "cuts" on the deconvolved spectra, before a final result is possible. In addition, the task of folding the uncertainties through the deconvolution process requires further work.

#### 4. Summary

Even though the results are still preliminary, the ATIC-2 spectra for H and He indicate an evolution of the spectral shape in the high energy region consistent with a changing energy dependence for the escape length in Leaky Box propagation. Adopting a particular diffusion model parameterization, the preliminary results can be reproduced if the source spectral indices for H and He differ by a small amount. Confirmation of these results is anticipated from an ATIC-3 balloon flight scheduled for 12/05 – 1/06 from McMurdo, Antarctica.

#### 5. Acknowledgements

The work was supported in Russia by the Russian Foundation for Basic Research grants Nos 02-02-16545 and 05-02-16222, in the US by NASA Supporting Research & Technology (NNG04WC12G, NNG04WC10G, NNG04WC06G) and in China by the Ministry of Science and Technology of China (2002CB713905, 2002AA732021, 2002AA732022).

#### References

- [1] T.G. Guzik et al., *Adv. Sp. Res.*, 33, 1763 (2004).
- [2] V.I. Zatsepin et al., *NIMA*, 524,195 (2004).
- [3] N.V. Sokolskaya et al., *Phys. At. Nucl.*, 68, 1176 (2005).
- [4] V.I. Zatsepin et al., *Proc. 28 ICRC*, 4, 1829 (2003).
- [5] H.S. Ahn et al., *Proc. 28 ICRC*, 4, 1833 (2003).
- [6] V.I. Zatsepin et al., *Izv. RAN, ser.fiz.*, 68, 1593 (2004).
- [7] J. Isbert et al., *This conference*.
- [8] K.E. Batkov et al., *This conference*.
- [9] A. Fasso et al., *Proc. Monte Carlo-2000 Conf. (Berlin, 2001, Springer-Verlag)*, p. 159 and p. 955.
- [10] S.P. Swordy, *24<sup>th</sup> ICRC*, 2, 697 (1995).
- [11] K. Asakimori et al., *Ap.J.*, 502, 278 (1998).
- [12] J.L. Osborne, V.S. Ptuskin, *Sov. Astron. Lett.*, 14 (2), (1988)
- [13] V.A. Derbina et al., *Ap. J. Lett.*, 628, L41 (2005).
- [14] J.J. Engelmann et al., *A&A*, 233, 96 (1990).
- [15] V.I. Zatsepin et al., *Phys. At. Nucl.*, 57, 645 (1994).
- [16] Y. Takahashi et al., *Nuci. Phys. B (Proc. Suppl.)* 60B, 83 (1998).
- [17] A.V. Apanasenko et al., *Astroparticle Physics.*, 16, 13 (2001).
- [18] M. Boezio et al., *Astroparticle Physics*, 19,583 (2003).
- [19] J. Alcaraz et al., *Phys. Lett. B* 490, 27 (2000); 494, 193 (2000).